

# Proton Transfer in Aminocyclopentadienyl Ruthenium Hydride Complexes

José A. Ayllon, Stephen F. Sayers, Sylviane Sabo-Etienne,\*  
Bruno Donnadiou, and Bruno Chaudret\*

Laboratoire de Chimie de Coordination CNRS, 205 Route de Narbonne,  
F-31077 Toulouse-Cedex 04, France

Eric Clot

Laboratoire de Structure et Dynamique des Systèmes Moléculaires et Solides,  
Case Courrier 14, Université de Montpellier 2, Place Eugène Bataillon,  
F-34095 Montpellier-Cedex, France

Received April 26, 1999

A new ruthenium hydride complex of the aminocyclopentadienyl ligand (Cp-N)RuH(PPh<sub>3</sub>)<sub>2</sub> (Cp-N = C<sub>5</sub>H<sub>4</sub>CH<sub>2</sub>CH<sub>2</sub>NMe<sub>2</sub>, **1**) has been prepared and characterized by X-ray diffraction. Protonation of **1** with excess HPF<sub>6</sub> leads to the dicationic derivative [(Cp-NH)RuH<sub>2</sub>(PPh<sub>3</sub>)<sub>2</sub>](PF<sub>6</sub>)<sub>2</sub> (**2**), in which both the metal and the amino substituent have been protonated. Addition of 1 equiv of HBF<sub>4</sub>·Et<sub>2</sub>O to **1** leads to the complex [(Cp-N)Ru(PPh<sub>3</sub>)<sub>2</sub>](BF<sub>4</sub>) (**3**), containing a chelating amino cyclopentadienyl ligand after elimination of H<sub>2</sub>. However, using (HNEt<sub>3</sub>)-(BPh<sub>4</sub>) or (HPBu<sub>3</sub>)(BPh<sub>4</sub>) as protonating agent, it is possible to form [(Cp-NH)RuH(PPh<sub>3</sub>)<sub>2</sub>](BPh<sub>4</sub>) (**4**), which was isolated as yellow crystals of **4**·H<sub>2</sub>O upon addition of undistilled methanol and characterized by X-ray crystallographic analysis. A fluxional process exchanging the ammonium proton and the hydride without changing the thermodynamic state of the system could be established by <sup>1</sup>H NMR, and activation energies of 11 kcal·mol<sup>-1</sup> were calculated for **4**·H<sub>2</sub>O and the product resulting from in situ addition of [HNEt<sub>3</sub>][BPh<sub>4</sub>] to **1**, whereas an activation energy of 10.1 kcal·mol<sup>-1</sup> was found for the product resulting from in situ addition of [HPBu<sub>3</sub>][BPh<sub>4</sub>] to **1**. A density functional study (B3PW91) was carried out, and the dihydrogen bond in the model system for **4** was calculated to be 1.545 Å, in excellent agreement with *T*<sub>1</sub> measurements (1.52 Å). The proposed mechanism for the fluxional process does not involve a proton transfer within the dihydrogen bond.

## Introduction

The presence of hydrogen bonds between a transition metal hydride and a hydrogen bond donor containing an O–H or an N–H group (dihydrogen bonds) has recently been established by Crabtree<sup>1</sup> and Morris<sup>2</sup> using various spectroscopic methods as well as solid-state structures. In these cases, intramolecular hydrogen bonding was rendered possible by the presence on the same complex of a hydride and a ligand containing the hydrogen bond donor. These structures seem adapted to proton transfer, and for instance, a dihydrogen tautomer has been proposed to be involved in the deuteration reaction of a complex containing a hydride

ligand hydrogen-bonded to the acidic proton of a thiolato pyridinium ligand.<sup>2a,d</sup> Intermolecular interactions were also evidenced by Crabtree in the solid state in an adduct of ReH<sub>5</sub>(PPh<sub>3</sub>)<sub>3</sub> with indole and in the H<sub>3</sub>NBH<sub>3</sub> adduct,<sup>3</sup> whereas Epstein and Berke<sup>4</sup> have identified such interactions in solution. Complexes displaying such hydrogen bonding have been proposed to be important intermediates for the protonation of hydrides or the reverse reaction, namely, the base-promoted heterolytic splitting of dihydrogen. In this respect, we have recently described the first observation of a reversible proton transfer between the dihydride complex *trans*-RuH<sub>2</sub>-(dppm)<sub>2</sub> involved in hydrogen bonding with hydrogen bond donors such as hexafluoro-2-propanol or phenols and a dihydrogen derivative.<sup>5</sup> We have furthermore demonstrated the influence of hydrogen bonding in solution on the magnitude of exchange couplings in

\* Corresponding author. Fax: (33) 5 61 55 30 03. E-mail: Chaudret@lcc-toulouse.fr.

(1) (a) Crabtree, R. H.; Siegbahn, P. E. M.; Eisenstein, O.; Rheingold, A.; Koetzle, T. F. *Acc. Chem. Res.* **1996**, *29*, 348. (b) Lee, J. C., Jr.; Peris, E.; Rheingold, A. L.; Crabtree, R. H. *J. Am. Chem. Soc.* **1994**, *116*, 11014. (c) Peris, E.; Lee, J. C., Jr.; Rambo, J. R.; Eisenstein, O.; Crabtree, R. H. *J. Am. Chem. Soc.* **1995**, *117*, 3845. (d) Peris, E.; Wessel, J.; Patel, B. P.; Crabtree, R. H. *J. Chem. Soc., Chem. Commun.* **1995**, 2175. (e) Yao, W.; Crabtree, R. H. *Inorg. Chem.* **1996**, *35*, 3007.

(2) (a) Lough, A. J.; Park, S.; Ramachandran, R.; Morris, R. H. *J. Am. Chem. Soc.* **1994**, *116*, 8356. (b) Park, S.; Ramachandran, R.; Lough, A. J.; Morris, R. H. *J. Chem. Soc., Chem. Commun.* **1994**, 2201. (c) Park, S.; Lough, A. J.; Morris, R. H. *Inorg. Chem.* **1996**, *35*, 3001. (d) Schlaf, M.; Lough, A. J.; Morris, R. H. *Organometallics* **1996**, *15*, 4423.

(3) (a) Wessel, J.; Lee, J. C., Jr.; Peris, E.; Yap, G. P. A.; Fortin, J. B.; Ricci, J. S.; Sini, G.; Albinati, A.; Koetzle, T. F.; Eisenstein, O.; Rheingold, A. L.; Crabtree, R. H. *Angew. Chem., Int. Ed. Engl.* **1995**, *34*, 2507. (b) Patel, B. P.; Yao, W.; Yap, G. P. A.; Rheingold, A. L.; Crabtree, R. H. *J. Chem. Soc., Chem. Commun.* **1996**, 991.

(4) Shubina, E. S.; Belkova, N. V.; Krylov, A. N.; Vorontsov, E. V.; Epstein, L. M.; Gusev, D. G.; Niedermann, M.; Berke, H. *J. Am. Chem. Soc.* **1996**, *118*, 1105.

(5) Ayllon, J. A.; Gervaux, C.; Sabo-Etienne, S.; Chaudret, B. *Organometallics* **1997**, *16*, 2000.

$\text{Cp}^*\text{RuH}_3(\text{PCy}_3)_6$  and used these modifications of exchange couplings to demonstrate the transfer of protons within a dihydrogen bond.<sup>6b</sup>

The existence of "dihydrogen bonds" having been established and the ease of proton transfer inside these associated structures having been demonstrated, it was interesting to try to study the proton transfer by imposing a geometry to the hydrogen bond through the design of the ligand sphere. Calculations by Akorta and Elguero have demonstrated the possibility of undergoing proton transfer in a strong electric field.<sup>7</sup> Jalon et al. have studied proton transfer in pyridylphenylphosphine ruthenium complexes and evidenced by saturation transfer the existence of an equilibrium between a proton linked to nitrogen and a hydride.<sup>8</sup> In our group we have chosen to use cyclopentadienyl ligands functionalized with amino groups.<sup>9</sup> Thus, the recent reports concerning the preparation on a multigram scale of sodium salts of amino-substituted cyclopentadienyl ligands,  $\text{NaCp-N}$  ( $\text{Cp-N} = \text{C}_5\text{H}_4\text{CH}_2\text{CH}_2\text{NMe}_2$ ,  $\text{C}_5\text{H}_4\text{CH}_2\text{CH}_2\text{CH}_2\text{NMe}_2$ ,  $\text{C}_5\text{H}_4\text{CH}(\text{CH}_2\text{CH}_2)_2\text{NMe}$ ) allowed an easy access to both the ligands and their metal complexes.<sup>10</sup> In previous studies we used piperidylcyclopentadienyl ligands. This led in iridium chemistry to the observation of dynamic equilibrium between a proton linked to the piperidyl moiety and two hydrides,<sup>11</sup> whereas in the ruthenium case, a so far not explained strong decrease of the relaxation time of the hydride (down to <2 ms) was found.<sup>12</sup> To build a more flexible system, we considered using cyclopentadienyl ligands accommodating linear amino groups such as  $\text{C}_5\text{H}_4\text{CH}_2\text{CH}_2\text{NMe}_2$  or  $\text{C}_5\text{H}_4\text{CH}_2\text{CH}_2\text{CH}_2\text{NMe}_2$ . However, during the course of this work, Lau and co-workers reported a very similar study involving these two ligands coordinated to a ruthenium hydrido dppm fragment.<sup>13</sup> In their case, they have been able to demonstrate by several techniques the presence of a hydrogen bond between a proton linked to the amine moiety and a hydride and to show the formation of a dicationic dihydrogen complex when using an excess of protonating agent. They have however not observed in their complex the hydride/proton exchange within the dihydrogen bond, nor could they obtain in this system the crystal structure of the monoprotonated species.

We report in this paper the synthesis of the new hydride complex  $(\text{Cp-N})\text{RuH}(\text{PPh}_3)_2$  ( $\text{Cp-N} = \text{C}_5\text{H}_4\text{CH}_2\text{CH}_2\text{NMe}_2$ ) (**1**) and its X-ray crystal structure and the

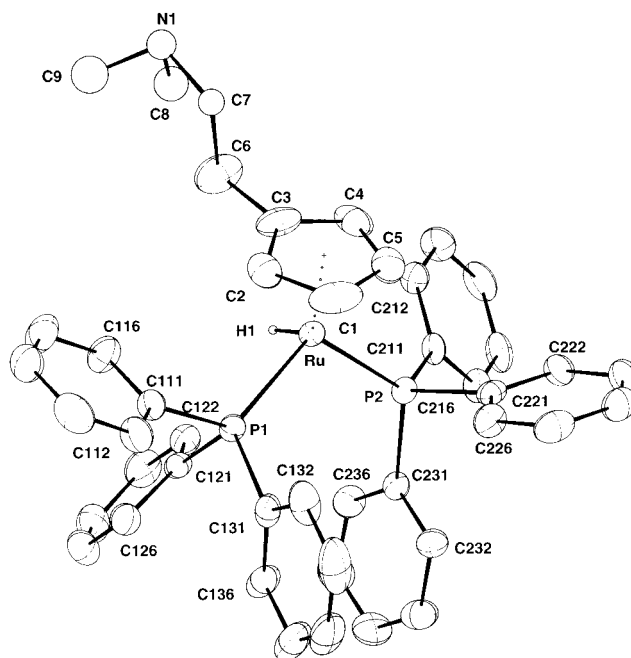


**Figure 1.** CAMERON view of  $(\text{C}_5\text{H}_4\text{CH}_2\text{CH}_2\text{NMe}_2)\text{RuH}(\text{PPh}_3)_2$  (**1**). Selected bond lengths (Å): Ru–H(1), 1.55(3); Ru–P(1), 2.2630(8); Ru–P(2), 2.2619(8); Ru–C(1), 2.250(3); Ru–C(2), 2.227(3); Ru–C(3), 2.239(4); Ru–C(4), 2.239(4); Ru–C(5), 2.245(4). Selected bond angles (deg): P(1)–Ru–P(2), 98.83(3); P(1)–Ru–H(1), 79.2(19); P(2)–Ru–H(1), 85.9(21).

protonation of **1**, leading, according to the protonation reagent, to chelation or formation of a novel hydride complex  $[(\text{Cp-NH})\text{RuH}(\text{PPh}_3)_2]\text{BPh}_4 \cdot \text{H}_2\text{O}$  (**4**), also characterized by X-ray crystallography. We also report the dynamic NMR spectra of the latter species. Moreover density functional calculations (B3PW91) have been carried out to characterize the conformation of the products and to elucidate the mechanism of the exchange process. With respect to the dppm system described by Lau and co-workers,<sup>13</sup> our experimental and theoretical study highlights the influence of any ligand modification (here phosphines) on these sensitive hydrogen-transfer processes.

## Results

**Synthesis and Characterization of the Neutral Complex 1.** The reaction of  $\text{RuH}(\text{OCOME})(\text{PPh}_3)_3$ <sup>14</sup> with  $\text{NaCp-N}$  in methanol at reflux for 45 min leads to the formation of  $(\text{Cp-N})\text{RuH}(\text{PPh}_3)_2$  (**1**), ( $\text{Cp-N} = \text{C}_5\text{H}_4\text{CH}_2\text{CH}_2\text{NMe}_2$ ) in 72% yield after appropriate workup. The complex was characterized by analytical and spectroscopic methods as well as by X-ray crystallographic analysis (see Figure 1). The most salient spectroscopic features are the observation in the <sup>1</sup>H NMR spectrum recorded in  $\text{CD}_2\text{Cl}_2$  of a hydride near –11 ppm ( $t$ ,  $J_{\text{P-H}}$  34 Hz), of two pseudotriplets for the cyclopentadienyl protons near 4.3 and 3.8 ppm, and of the methyl groups attached to nitrogen near 2.1 ppm, as well as the observation in the <sup>31</sup>P NMR spectrum of a singlet at 70.1 ppm. Other <sup>1</sup>H and <sup>13</sup>C NMR data are given in the Experimental Section. The infrared spectrum recorded

(6) (a) Ayllon, J. A.; Sabo-Etienne, S.; Chaudret, B.; Ulrich, S.; Limbach, H.-H. *Inorg. Chim. Acta* **1997**, *259*, 1. (b) Gründemann, S.; Ulrich, S.; Limbach, H.-H.; Golubev, N. S.; Denisov, G. S.; Epstein, L.; Sabo-Etienne, S.; Chaudret, B. *Inorg. Chem.* **1999**, *38*, 2550.

(7) Rozas, I.; Akorta, I.; Elguero, J. *Chem. Phys. Lett.* **1997**, *275*, 423.

(8) Caballero, A.; Jalon, F. A.; Manzano, B. R. *J. Chem. Soc., Chem. Commun.* **1998**, 1879.

(9) (a) Jutzi, P.; Siemeling, U. *J. Organomet. Chem.* **1995**, *500*, 175. (b) Jutzi, P.; Bangel, M.; Neumann, B.; Stammel, H.-G. *Organometallics* **1996**, *15*, 4559, and references therein.

(10) (a) MacGowan, P. C.; Hart, C. E.; Donnadiou, B.; Poilblanc, R. *J. Organomet. Chem.* **1997**, *528*, 191. (b) Philippopoulos, A. I.; Hadjiladis, N.; Hart, C. E.; Donnadiou, B.; MacGowan, P. C.; Poilblanc, R. *Inorg. Chem.* **1997**, *36*, 1842.

(11) Abad, M. M.; Atheaux, I.; Maisonnat, A.; Chaudret, B. *Chem. Commun.* **1999**, 381.

(12) Castellanos, A.; Ayllon, J. A.; Sabo-Etienne, S.; Donnadiou, B.; Chaudret, B.; Yao, W.; Kavallieratos, K.; Crabtree, R. H. *C.-R. Acad. Sci., Ser. IIc* **1999**, 359.

(13) Chu, H. S.; Lau, C. P.; Wong, K. Y.; Wong, W. T. *Organometallics* **1998**, *17*, 2768.

(14) Mitchel, R. W.; Spencer A.; Wilkinson G. *J. Chem. Soc., Dalton Trans.* **1973**, 846.

**Table 1. Crystal Data for 1 and 4**

	C <sub>45</sub> H <sub>45</sub> NP <sub>2</sub> Ru (1)	[C <sub>45</sub> H <sub>46</sub> NP <sub>2</sub> Ru][B(C <sub>6</sub> H <sub>5</sub> ) <sub>4</sub> ]·H <sub>2</sub> O (4)
fw	762.79	1085.14
$\rho_{\text{calcd}}$ (g·cm <sup>-3</sup> )	1.34	1.27
$\mu$ (cm <sup>-1</sup> )	5.26	3.67
F <sub>000</sub>	769.62	2299.35
crystal system	monoclinic	monoclinic
space group	<i>Pc</i>	<i>P2<sub>1</sub>/c</i>
<i>a</i> (Å)	9.8147(8)	30.462(4)
<i>b</i> (Å)	10.030(1)	10.381(1)
<i>c</i> (Å)	19.316(2)	18.175(3)
$\beta$ (deg)	100.901(9)	100.24(2)
<i>V</i> (Å <sup>3</sup> )	1867	5656
<i>Z</i>	2	4
crystal size	0.3 × 0.3 × 0.2	0.2 × 0.1 × 0.07
crystal color	light yellow	yellow
radiation type	Mo K $\alpha$	Mo K $\alpha$
wavelength (Å)	0.71073	0.71073
temp (K)	160	140
2 $\theta$ range (deg)	2.9–48.4	2.3–42.0
no. of measured reflns	14534	23673
no. of indep reflns	5531	5872
no. of reflns used [ <i>I</i> > 3 $\sigma$ ( <i>I</i> )]	5208	3182
<i>R</i>	0.026	0.054
<i>R<sub>w</sub></i>	0.032	0.048
GOF	0.7	1.2

on a sample dispersed in Nujol shows the frequency of the Ru–H stretch at 1941 cm<sup>-1</sup>. The X-ray crystal structure of **1** is shown in Figure 1 (see Table 1). The Ru–H distance is equal to 1.55(3) Å, whereas no significant change induced by the presence of the amino group was observed for the other distances compared to CpRuCl(PPh<sub>3</sub>)<sub>2</sub>.<sup>15</sup>

**Protonation of 1. Protonation with Excess HPF<sub>6</sub>.** Protonation of **1** with excess HPF<sub>6</sub>·H<sub>2</sub>O in methanol at room temperature leads to the dicationic derivative [(Cp-NH)RuH<sub>2</sub>(PPh<sub>3</sub>)<sub>2</sub>](PF<sub>6</sub>)<sub>2</sub> (**2**) isolated in 69% yield and in which both the metal and the amine moiety have been protonated. Interestingly, this reaction produces exclusively the dihydride isomer, as deduced from the observation of a triplet near -7.4 ppm (*J<sub>P-H</sub>* 24.0 Hz) for the hydrides in the <sup>1</sup>H NMR spectrum. The protonation of the amino group is apparent by the downfield shift of the methyl groups to ca. 2.8 ppm and by the observation of the proton linked to nitrogen at 6.6 ppm. Other interesting spectroscopic features are an AA'BB' pattern for the Cp protons at 5.08 and 4.81 ppm and the shift of the <sup>31</sup>P NMR signal near  $\delta$  61 ppm.

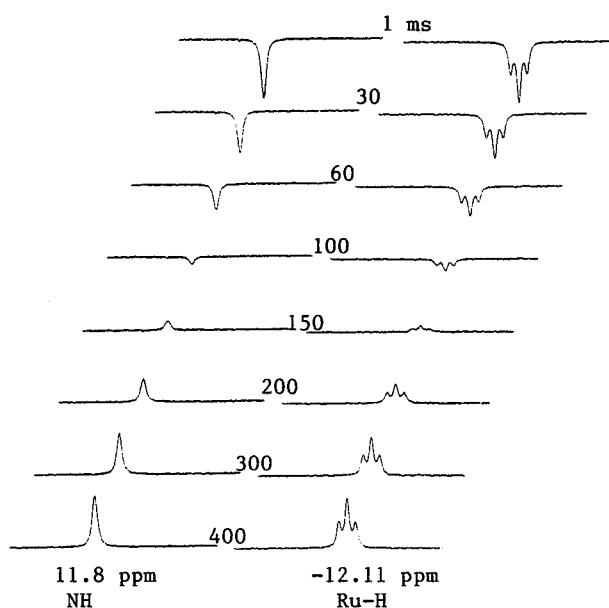
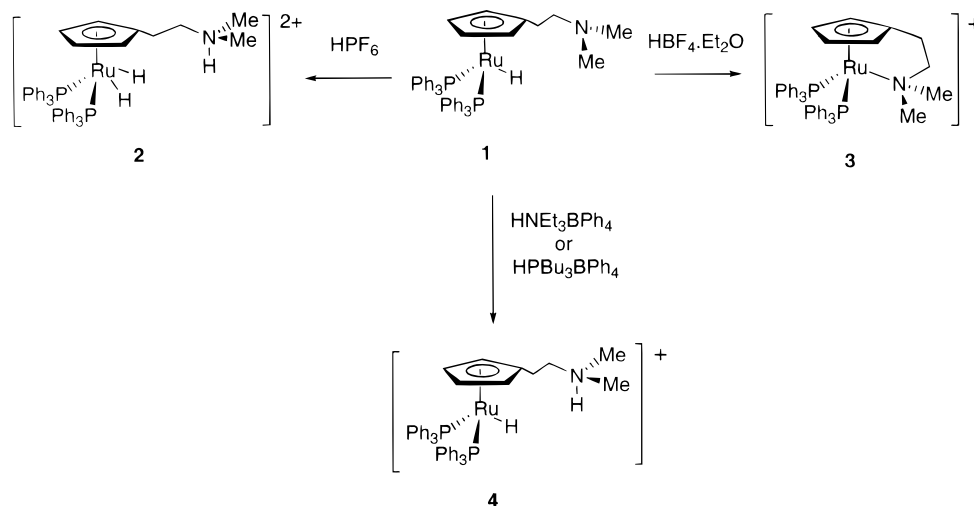
**Protonation of 1 with Stoichiometric Amounts of HBF<sub>4</sub>·Et<sub>2</sub>O (Scheme 1).** Upon protonation of **1** with stoichiometric amounts of HBF<sub>4</sub>·Et<sub>2</sub>O in diethyl ether, a new complex, namely, [(Cp-N)Ru(PPh<sub>3</sub>)<sub>2</sub>](BF<sub>4</sub>) (**3**), accommodating a chelating amino cyclopentadienyl ligand, was prepared, together with traces (ca. 1%) of the diprotonated [(Cp-NH)Ru(H)<sub>2</sub>(PPh<sub>3</sub>)<sub>2</sub>](BF<sub>4</sub>)<sub>2</sub>, similar to **2**, as deduced from the observation in <sup>1</sup>H NMR of a hydride signal at -7.33 ppm (*J<sub>P-H</sub>* 24 Hz). <sup>1</sup>H NMR data of the major product show no hydride signal but a significant modification of the chemical shift of the cyclopentadienyl protons compared to **1**, which resonate at 4.65 and 3.57 ppm, whereas the methyl groups on

nitrogen resonate at 2.73 ppm. The <sup>31</sup>P NMR spectrum shows a singlet at 64.62 ppm. The mechanism of this reaction probably involves protonation of the hydride and fast elimination of dihydrogen. The driving force is most probably the formation of a stable five-membered ring, many examples of which have been reported. These points will be illustrated in the theoretical section.

**Proton Transfer by Ammonium or Phosphonium Salts.** The reaction of **1** with (HNEt<sub>3</sub>)(BPh<sub>4</sub>) was first studied in situ in an NMR tube. In contrast to the reaction with HBF<sub>4</sub>, no dihydrogen elimination is observed when the reaction is carried out at room temperature, but a new complex is formed: **4**·NEt<sub>3</sub>, corresponding to **1** + (HNEt<sub>3</sub>BPh<sub>4</sub>). At room temperature, the signals in the <sup>1</sup>H NMR spectrum at 4.57 and 3.53 ppm, due to the Cp protons, are shifted compared to those of **1** and close to the position of the signals of the Cp protons of **3**, whereas the amino methyl groups resonate at 2.06 ppm, i.e., close to the position of those of **1**. The <sup>31</sup>P NMR spectrum displays a single resonance near 66 ppm. The most interesting spectroscopic feature is the presence of a very broad peak centered at -0.95 ppm, which integrates for two protons in the <sup>1</sup>H NMR spectrum (200 MHz). At 400 MHz and 193 K, two broad peaks are observed at -11.68 and +11.9 ppm, respectively, due to a hydride and an ammonium proton. When the temperature is slowly increased, the high-field peak broadens up to a temperature of 253 K, after which it is no longer visible. The low-field peak shifts to higher field as the temperature rises and also disappears at a temperature higher than 253 K. At room temperature, no signal is visible because of the coalescence. An increase in temperature could not be carried out because of decomposition of the product, but as stated above, upon lowering the field of observation (200 MHz), the coalescence peak is observed at -0.95 ppm. The system is fully reversible. This observation indicates the presence of a two-site exchange between two protons on the NMR time scale. One is a hydride, whereas the other is an ammonium proton, hence indicating that protonation of the complex has occurred. The energy of activation of the process, derived from the coalescence temperature, was found to be 11 kcal·mol<sup>-1</sup>. This process is only a two-site exchange and not a thermodynamic proton transfer. No formation of a dihydride, of a dihydrogen complex or of the chelate complex **3** was observed.

We chose to carry out the same reaction with (HPBu<sub>3</sub>)-(BPh<sub>4</sub>) since the <sup>1</sup>H-<sup>31</sup>P coupling could give us a supplementary tool to characterize the proton exchange. The in situ reaction with **1** produces a complex very similar but not identical to the previous one, **4**·PBu<sub>3</sub> corresponding to **1** + (HPBu<sub>3</sub>BPh<sub>4</sub>). For example the Cp protons resonate at 4.72 and 3.33 ppm and the methyl groups attached to nitrogen at 2.09 ppm. A broad peak is observed at room temperature at -0.3 ppm (400 MHz, CD<sub>2</sub>Cl<sub>2</sub>) for the rapidly exchanging signals of the hydride and of the proton attached to nitrogen. At low temperature (<233 K) this signal splits into two signals observed at 11.7 and -12.1 ppm and attributed respectively to the N–H proton and to the hydride. Both signals remain in slow exchange since they display the same relaxation time; this is obvious in Figure 2, which shows the inversion recovery spectra of **1** + (HPBu<sub>3</sub>-BPh<sub>4</sub>) at 213 K and 400 MHz. The barrier of activation

(15) Bruce, M. I.; Wong, F. S.; Skelton, B. W.; White, A. H. *J. Chem. Soc., Dalton Trans.* **1981**, 1398.

Scheme 1. Protonation Reactions of **1**

**Figure 2.** Inversion recovery spectra of **1** + (HPBu<sub>3</sub>BPh<sub>4</sub>) at 213 K and 400 MHz, showing the low-field amino proton and the high-field hydride resonances. The delay times shown are in ms.

of the process was calculated to be 10.1 kcal·mol<sup>-1</sup>, slightly lower than in the case of **1** + (HNEt<sub>3</sub>BPh<sub>4</sub>). The absence of H–P coupling in <sup>1</sup>H and <sup>31</sup>P NMR spectra of the PBu<sub>3</sub> group demonstrates that the proton has been transferred from phosphorus to nitrogen. However, a fluxional process is visible by <sup>31</sup>P NMR spectroscopy at higher temperatures. The peak attributed to PBu<sub>3</sub> at –29 ppm disappears at temperatures higher than 263 K, suggesting the involvement of this molecule in the fluxional proton-transfer process. A low *T*<sub>1</sub> minimum value (130 ms, 400 MHz) was observed for both the hydride and the ammonium proton in this system. Using **1** as a reference for all relaxation effects besides the dihydrogen bond and a methodology previously described, we can calculate an approximate value of the H···H separation (1.52 Å) which is consistent with the presence of a dihydrogen bond in solution.<sup>16</sup>

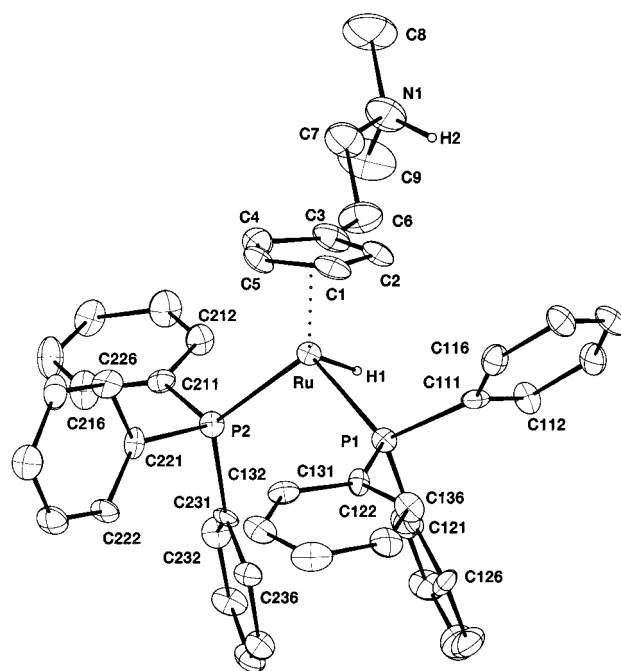


**Figure 3.** CAMERON view of [(C<sub>5</sub>H<sub>4</sub>CH<sub>2</sub>CH<sub>2</sub>NHMe<sub>2</sub>)RuH(PPh<sub>3</sub>)<sub>2</sub>](BPh<sub>4</sub>)·H<sub>2</sub>O (**4**·H<sub>2</sub>O). Selected bond lengths (Å): Ru–H(1), 1.58(13); Ru–P(1), 2.248(2); Ru–P(2), 2.270(2); Ru–C(1), 2.244(7); Ru–C(2), 2.235(8); Ru–C(3), 2.239(7); Ru–C(4), 2.238(8); Ru–C(5), 2.287(8); N(1)–H(2), 1.02(3). Selected bond angles (deg): P(1)–Ru–P(2), 100.75(7); P(1)–Ru–H(1), 80.6(45); P(2)–Ru–H(1), 94.5(46).

It was not possible to isolate pure any complex incorporating the triethylamine or tributylphosphine molecules. However addition of diethyl ether to a dichloromethane reaction solution of **1** + HPBu<sub>3</sub>BPh<sub>4</sub> or **1** + HNEt<sub>3</sub>BPh<sub>4</sub> leads to the precipitation of powders, which from NMR and microanalytical data definitely incorporate the phosphine or amine ligand. After several attempts, crystals could be grown from dichloromethane/wet methanol, leading to [(Cp–NH)RuH(PPh<sub>3</sub>)<sub>2</sub>](BPh<sub>4</sub>)·H<sub>2</sub>O (**4**·H<sub>2</sub>O) and characterized by X-ray diffraction (see Figure 3 and Table 1). The structure shows a single Ru–H(1) bond (1.58(13) Å) and a N–H(2) bond (1.02(3) Å) in agreement with the exclusive protonation of the amine moiety. No hydrogen bonding, whether inter- or intramolecular, is present in the structure. All

(16) Moreno, B.; Sabo-Etienne, S.; Chaudret, B.; Rodriguez, A.; Jalon, F.; Trofimenko, S. *J. Am. Chem. Soc.* **1995**, *117*, 7441.

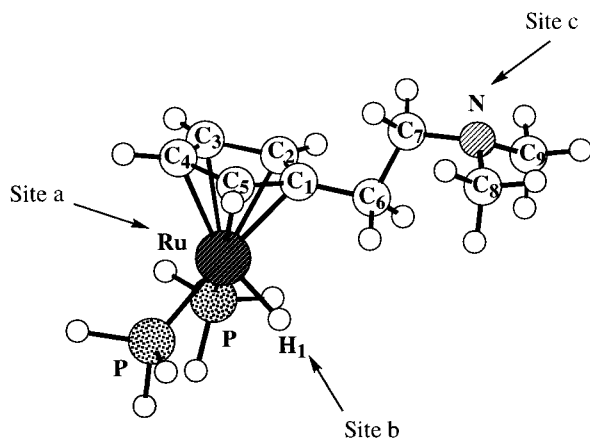


**Figure 4.** Calculated (B3PW91) geometry for **A** showing the atom labeling and the various possible sites for protonation. Selected bond lengths (Å): Ru–P, 2.260; Ru–H(1), 1.612; Ru–C(1), 2.274; Ru–C(2), 2.255; Ru–C(3), 2.292; C(1)–C(6), 1.498; C(6)–C(7), 1.547; C(7)–N, 1.454. Selected bond angles (deg): P–Ru–P, 92.0; P–Ru–H(1), 81.4; C(1)–C(6)–C(7), 111.3; C(6)–C(7)–N, 116.9.

the other distances and angles are typical of such half-sandwich complexes. The NMR spectra of crystals of **4**·H<sub>2</sub>O are totally similar to those of the mixture **1** + HNEt<sub>3</sub>BPh<sub>4</sub>. This could indicate that neither triethylamine nor water plays a role in the exchange process even if either of these bases is present in the solid-state structure of **4** or, more likely, that they play a similar role, i.e., give additional hydrogen bonding to the ammonium proton, thus preventing the transfer and dihydrogen elimination and/or favoring the exchange process proposed in the theoretical section (vide infra). In the case of the mixture **1** + HPBu<sub>3</sub>BPh<sub>4</sub>, we observe an easier proton/hydride exchange as well as the disappearance of the PBu<sub>3</sub> signal above 263 K, in agreement with the involvement of the additional base in the proton-transfer process through hydrogen bonding or transient re-formation of a phosphonium salt.

**Theoretical Calculations. Structure of the Monohydride.** The optimized geometry for the model compound RuH(PH<sub>3</sub>)<sub>2</sub>(Cp-N), **A** (Cp-N = C<sub>5</sub>H<sub>4</sub>CH<sub>2</sub>CH<sub>2</sub>NMe<sub>2</sub>) (Figure 4), is in very good agreement with the X-ray structure obtained for RuH(PPh<sub>3</sub>)<sub>2</sub>(Cp-N), **1** (Figure 1 and Supporting Information). The bonding of the substituted Cp ring is well described, although the calculated Ru–C bond distances are slightly longer than the experimental ones. However the trend among the three different bonds (Ru–C<sub>1</sub>, Ru–C<sub>2</sub>, and Ru–C<sub>3</sub>) is correctly reproduced. The computed Ru–P bond distance is in excellent agreement with the experimental value, and the calculated smaller P–Ru–P angle (92.1° vs 98.83°) is due to the nature of the model phosphine PH<sub>3</sub>, which underestimates the steric repulsion between the substituents on the phosphorus atoms. The calculated Ru–H<sub>1</sub> distance of 1.612 Å is typical of ruthenium–hydride distances computed by density functional theory and compares very well with experimental value.<sup>17</sup>

The amino chain on the Cp ring is also qualitatively well described with, however, two discrepancies among the C–C bond distances. The C<sub>1</sub>–C<sub>6</sub> and C<sub>6</sub>–C<sub>7</sub> bond distances are calculated to be smaller than the experimental ones by 0.1 Å. Nevertheless the three angles (Ru–C<sub>1</sub>–C<sub>6</sub>, C<sub>1</sub>–C<sub>6</sub>–C<sub>7</sub>, and C<sub>6</sub>–C<sub>7</sub>–N) describing the

orientation of the chain with respect to the ruthenium center do compare very well with the experimental data.

**Protonation of the Monohydride.** In complex **A**, there are three different basic sites that can react with an acid and yield a cationic species (Figure 5). Protonation at site **a** yields a trans dihydride complex **Ba**, whose optimized geometry is given in the Supporting Information along with some geometrical parameters. The two Ru–H bond distances are typical for ruthenium hydrides (1.612 and 1.606 Å). The particular geometrical feature of **Ba** is the larger angle between the two phosphorus atoms as a consequence of the trans geometry of the hydrides (92.1° for **A** vs 102.6° for **Ba**). This type of structure would thus be very difficult to obtain with chelating diphosphine because the P–Ru–P angle is constrained to remain below a certain value.

Protonation at site **b** yields a dihydrogen complex **Bb** with a H–H bond distance of 0.879 Å (Supporting Information). As expected, the P–Ru–P angle is not very large (90.9°), and this kind of structure could be observed with a chelating diphosphine like dpmm.<sup>13</sup> Finally, protonation at site **c** yields the ammonium complex **Bc** with a typical N–H bond distance (1.023 Å), and the P–Ru–P angle has not varied much (91.2°), which indicates that this structure could also be obtained with a chelating diphosphine.

The most stable of the three structures shown in Figure 5 is **Bb**, with **Bc** lying only at 0.3 kcal·mol<sup>−1</sup> above **Bb** and **Ba** lying at 2.6 kcal·mol<sup>−1</sup> above **Bb**. There is thus not a strong thermodynamic preference for one site of protonation. The higher energy of **Ba** may be due to the more important geometrical reorganization required and especially the opening of the P–Ru–P angle. However this difference is not very important, and we cannot rationalize the differences observed experimentally for **1** when it is reacted with either HBF<sub>4</sub> or HNEt<sub>3</sub> by just looking at the relative stability of **Ba**, **Bb**, and **Bc**.

**Formation of the Chelate Complex.** Reaction of **1** with HBF<sub>4</sub> yields the complex [(Cp-N)Ru(PPh<sub>3</sub>)<sub>2</sub>](BF<sub>4</sub>), **3**, containing a chelating amino cyclopentadienyl ligand. We have optimized the model compound [(Cp-N)Ru(PH<sub>3</sub>)<sub>2</sub>]<sup>+</sup>, **C**, with a chelating amino chain on the Cp ring (Supporting Information). The geometrical parameters for **C** compare very well with the geometry of the related complex [(Cp-N)Ru(dpmm)]<sup>+</sup> published by Lau and co-workers.<sup>13</sup> The system {**C** + H<sub>2</sub>} is 2.6 kcal·mol<sup>−1</sup> less stable than the dihydrogen complex **Bb**, indicating that the later might be observed by protonation at very low temperature. However the chelate compound is entropically favored with increasing temperature.

There are several possible conformations for the CH<sub>2</sub>–CH<sub>2</sub>NMe<sub>2</sub> chain on the Cp ring. The conformation corresponding to the chelate system is a priori energetically not favored. For the monohydride **A** this kind of conformation is 18.1 kcal·mol<sup>−1</sup> less stable than the conformation shown in Figure 1, while for **Bb** it is 7.4 kcal·mol<sup>−1</sup> less stable (**Bb** vs **Bb'** in Figure 6). Cp rings

(17) (a) Coalter, J. N., III; Spivak, G. J.; Gérard, H.; Clot, E.; Davidson, E. R.; Eisenstein, O.; Caulton, K. G. *J. Am. Chem. Soc.* **1998**, *120*, 9388. (b) Rodriguez, V.; Sabo-Etienne, S.; Chaudret, B.; Thoburn, J.; Ulrich, S.; Limbach, H.-H.; Eckert, J.; Barthelat, J.-C.; Hussein, K.; Marsden, C. J. *Inorg. Chem.*, **1998**, *37*, 3475. (c) Delpech, F.; Sabo-Etienne, S.; Daran, J.-C.; Chaudret, B.; Hussein, K.; Marsden, C. J.; Barthelat, J.-C. *J. Am. Chem. Soc.* **1999**, *121*, 6668.

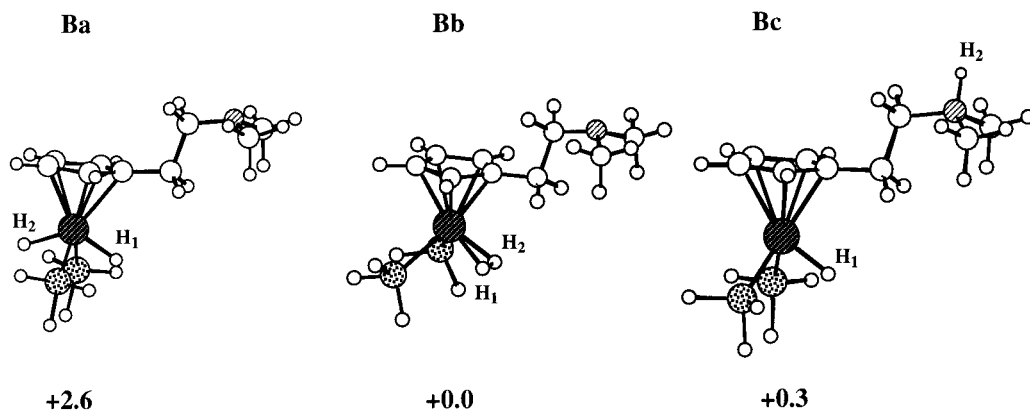


**Figure 5.** Calculated geometries and relative energies (kcal·mol<sup>-1</sup>) for the products (**Ba**, **Bb**, and **Bc**) resulting from protonation of **A**.

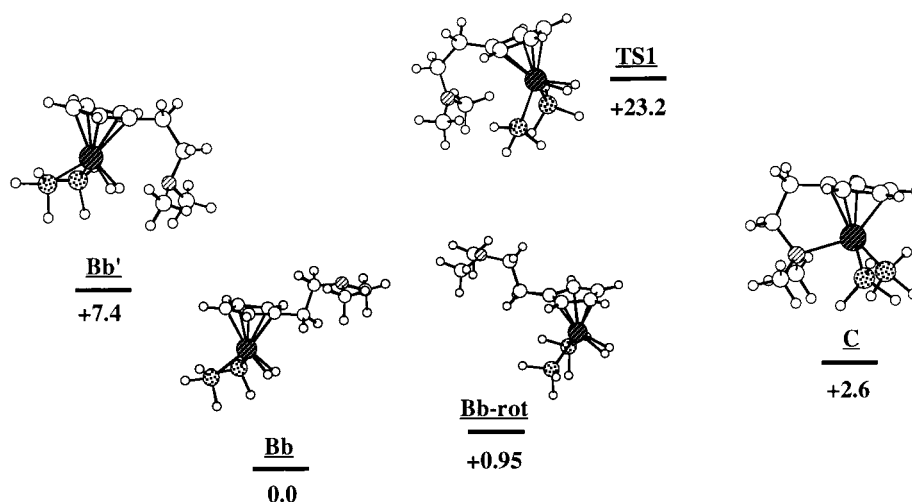


**Figure 6.** Mechanism for the formation of the chelate complex **C** from the protonated complex **Bb** (relative energies in kcal·mol<sup>-1</sup>).

are known to be fluxional, and rotation leading to structures such as **Bb-rot** (Figure 6) can be obtained easily. The computed energy difference is only 0.95 kcal·mol<sup>-1</sup> between **Bb** and **Bb-rot**.

The chelate complex is then formed by substitution of the H<sub>2</sub> ligand by the amino group through a transition state **TS1** (Figure 6) lying at 23.2 kcal·mol<sup>-1</sup> above **Bb**. In the transition state, the nitrogen atom is in a planar configuration with the perpendicular p orbital pointing toward the metal center. The P–Ru–P angle of 90.6° is not very large, and this mechanism might also be operative with a chelating diphosphine although certainly less easy.

**Formation of a Dihydrogen Bond.** When the protonation occurs at site **c**, the complex obtained **Bc** is not the most stable conformation and the amino chain prefers to adopt a geometry where it is pointing toward the ruthenium center. The optimized geometry for this complex **D** is shown in Figure 7, and it is 7.1 kcal·mol<sup>-1</sup> more stable than **Bc**, in apparent contradiction with the X-ray crystal structure for **4** (see Figure 3). However, the energy differences between the two structures are very small, which may explain that the crystal packing imposes the observed geometry. The main characteristic of this structure is the presence of a dihydrogen bond between the hydride and the hydrogen atom bound to nitrogen. The distance between the two hydrogen nuclei (1.545 Å) is in very good agreement with the value

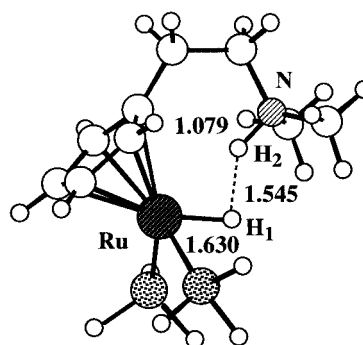


**Figure 7.** Calculated geometry for the complex **D** with the dihydrogen bond (distances in Å).

obtained from relaxation time measurements. As a consequence of the interaction between the two hydrogen atoms, the N–H bond is significantly elongated (1.079 Å).

**Exchange of the Two Hydrogen Atoms.** The two hydrogen atoms involved in the dihydrogen bond are equivalent ( $\delta \approx 0$  ppm) at room temperature on the NMR spectra, but they decoalesce at 253 K to give two peaks ( $\delta \approx -12$  ppm and  $\delta \approx 12$  ppm). The activation energy for the fluxional process was calculated to be around 11 kcal·mol<sup>-1</sup> depending of the acid used for the protonation (HNEt<sub>3</sub><sup>+</sup> or HPBu<sub>3</sub><sup>+</sup>). Usually it is assumed

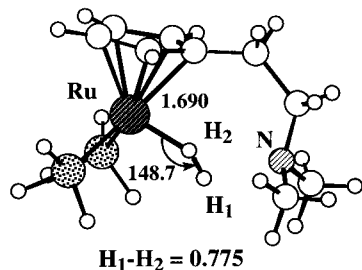


**Figure 8.** Calculated geometry for the transition state between the chelate complex **C** and the complex **D** with the dihydrogen bond (distances in Å).

for this kind of fluxional process that a dihydrogen complex is formed as an intermediate. The rotation of the  $H_2$  ligand in this complex accomplishes the exchange of the two hydrogen atoms. In the present study we have not been able to obtain complex **4** by reaction of **3** with  $H_2$ , nor have we been able to extrude  $H_2$  from **4** to obtain **3**. The chemistry of the chelate complex is thus apparently disconnected from the chemistry of the complex with the dihydrogen bond. As a dihydrogen complex is involved in the formation of the chelate complex (Figure 6), such species cannot be present along the path for the formation of complex **4**; otherwise it would be possible to go easily from **3** to **4** and vice versa.

In fact we have optimized the transition state connecting the two complexes **C** and **D**, and it is a  $\eta^1$  dihydrogen complex (Figure 8) lying at  $37.2 \text{ kcal}\cdot\text{mol}^{-1}$  above **D**. The H–H bond distance of  $0.775 \text{ \AA}$  is short for a dihydrogen complex because the  $\eta^1$  binding mode does not allow for an efficient back-donation from the metal that would result in a longer H–H bond. The Ru–H–H angle of  $148.7^\circ$  is also not common for a dihydrogen complex, and the  $\eta^1$  mode of coordination explains the high energy of this structure. The synergy between  $\sigma$  donation and  $\pi$  back-donation is not favored, and the binding of  $H_2$  is consequently less strong. This explains why it is difficult to go chemically from **3** to **4**, although the difference in energy between **D** and  $\{\mathbf{C} + H_2\}$  is only  $9.4 \text{ kcal}\cdot\text{mol}^{-1}$  (**D** is the most stable).

Although we have not characterized any transition state corresponding to the exchange of the two hydrogen atoms, we propose a possible mechanism for the exchange. This mechanism originates from the observation that no trans dihydride with the amino chain pointing toward one H could have been optimized. Despite all our attempts, we always observed transfer of one of the two hydrides to the nitrogen atom. The optimized structure for this complex **E** is lying only  $4.7 \text{ kcal}\cdot\text{mol}^{-1}$  above **D**, and Figure 9 shows in a pictorial way the proposed mechanism. The hydrogen atom initially on the nitrogen ( $H$ ) is transferred to the metal in several steps.

First the dihydrogen bond is broken to give the protonated complex **Bc**. The Cp ring can easily rotate and the complex **Bc-rot** is obtained, which lies  $1.7 \text{ kcal}\cdot\text{mol}^{-1}$  above **Bc**. As in the case of the compound **D** with the dihydrogen bond, complex **E** with the amino chain pointing toward the metal is more stable by  $4.1 \text{ kcal}\cdot\text{mol}^{-1}$  than the structure **Bc-rot** with the chain pointing away from Ru. This might be due to a stabilizing interaction between the hydrogen atom bound to N and the ruthenium center.

From this complex **E** the hydrogen atom ( $H$ ) can be transferred to the metal through a transition state that we have not been able to locate. This step would most probably be the rate-determining step and would account for the observed activation energy of ca.  $11 \text{ kcal}\cdot\text{mol}^{-1}$ , which is expected to be significantly influenced by the presence of a base ( $H_2O$ ,  $NEt_3$ ,  $PBu_3$ ). A geometry corresponding to a hydrogen atom between N and Ru was calculated to be less stable than **D** by only  $15 \text{ kcal}\cdot\text{mol}^{-1}$ ; however despite all our attempts we failed to optimize this structure as a transition state.

From **Bc** it is now straightforward to consider the inverse mechanism working again after rotation of the Cp ring to take the other hydrogen atom from the metal and to create a new dihydrogen bond where the two hydrogen atoms have been permuted.

## Discussion

We describe in this study the synthesis of a new ruthenium hydride complex containing an aminocyclopentadienyl ligand (**1**). This compound contains three basic sites, namely, the metal, the hydride, and the amino group, each one able to react or to undergo hydrogen bonding with an electrophile (in this case the proton). It is possible to add two protons to it, which leads to the dicationic dihydride derivative (**2**) containing a quaternary ammonium substituent on the cyclopentadienyl rings. Such dicationic electrophilic hydride complexes may display interesting catalytic properties and may even be soluble in water. The reactivity of **2** was not studied for the present report but is now under investigation. Nevertheless, **2** represents the final thermodynamic state of the system and gives us a reference for the present study.

Addition of a strong acid such as  $HBF_4\cdot Et_2O$  to **1** leads to **3** after evolution of dihydrogen and chelation of the aminocyclopentadienyl ligand, whereas the use of softer acids such as  $HNEt_3BPh_4$  or  $HPBu_3BPh_4$  allows the isolation of **4**, in which only the amine moiety of the aminocyclopentadienyl ligand is protonated. The theoretical calculations at the DFT level demonstrate that this is not due to a thermodynamic preference for the chelate system. It has previously been shown that the kinetic site of protonation of complexes such as  $CpRuH(PR_3)_2$  is the hydride, hence leading to a dihydrogen complex.<sup>18</sup> In the present case, elimination of dihydrogen is driven by the formation of kinetically inert chelate complex **3**. In the presence of a weaker acid, or perhaps for steric reasons because of the size of the ammonium or phosphonium cation, the protonation occurs on the nitrogen of the pendent amino group to give **4** and does not lead to the protonation of the hydride. A process exchanging the hydride with the ammonium proton and involving an activation energy of  $10\text{--}11 \text{ kcal}\cdot\text{mol}^{-1}$  (according to the systems) has been evidenced by variable-temperature NMR experiments. It is interesting to note that **3** and **4** are both stable and that they do not interconvert. **3** does not react with  $H_2$  in mild conditions, whereas **4** does not lose  $H_2$  at room temperature in solution.

DFT calculations show that the presence of a dihydrogen bond associating the hydride and the ammonium

(18) (a) Jessop, P. G.; Morris, R. H. *Coord. Chem. Rev.* **1992**, *121*, 155. (b) Heinekey, D. M.; Oldham, W. J., Jr. *Chem. Rev.* **1993**, *93*, 913.

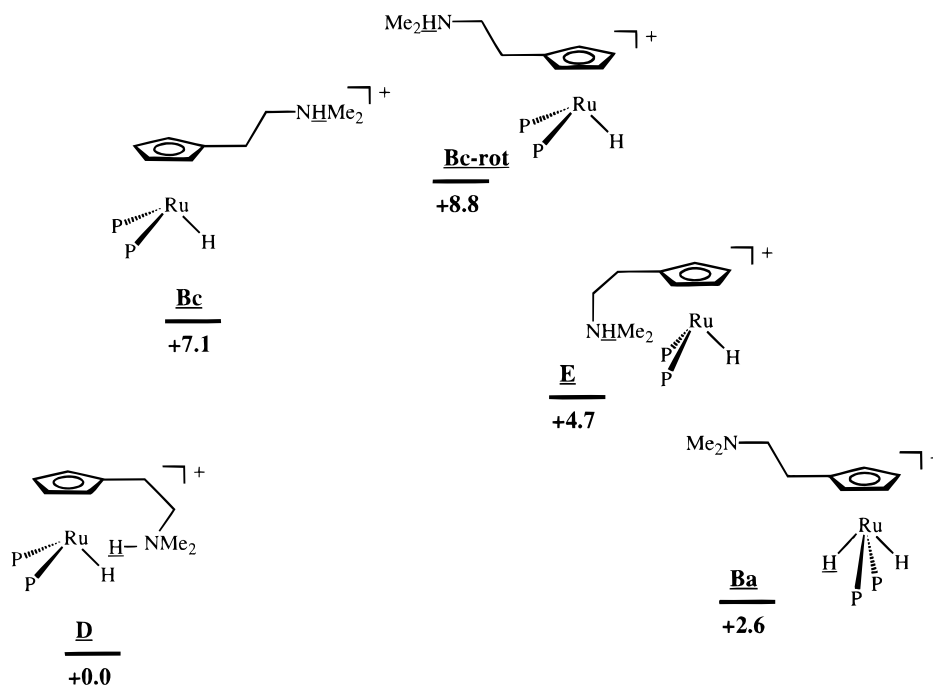


**Figure 9.** Proposed mechanism for the intramolecular exchange of the two hydrogen atoms involved in the dihydrogen bond (relative energies in kcal·mol<sup>-1</sup>).

proton in **D** (model for **4**) is favored by 7.1 kcal·mol<sup>-1</sup> over the open structure **Bc**. This is in agreement with the observation of a low  $T_1$  minimum value (130 ms, 400 MHz) observed for both the hydride and the ammonium proton in the case of the reaction of **1** + HPBu<sub>3</sub>BPh<sub>4</sub>, which is consistent with the presence of such a dihydrogen bond in solution and a short hydride/proton separation (1.52 Å). However, the crystal structure evidences the presence in the solid state of a conformation in which no interaction is present between the proton on nitrogen and the hydride. Moreover, the ammonium proton is not involved in any other hydrogen-bonding interaction, in apparent contradiction with the fact that, at least in the phosphonium case, the presence of an additional base will play a role in the exchange process between the hydride and the ammonium proton. The latter assumption derives from the broadening of the phosphine NMR signal during the exchange process and from the fact that the activation energy of the process is lower in the presence of PBu<sub>3</sub>. It is possible that, as proposed in the theoretical section, the rate-determining step is the transfer of proton from the ammonium to ruthenium and back and that this process is assisted by an additional base present in the vicinity.

All these observations and calculations lead us to propose a new mechanism for the exchange process between the hydride and the ammonium proton which does not involve proton transfer within the dihydrogen bond (see Figure 9). Whereas in the solid state no dihydrogen bond is present, it is likely that in solution several fluxional pathways are present, one of which will lead to the thermodynamically most stable species which contains a dihydrogen bond between the hydride and the ammonium proton. The lifetime of this species is presumably significant enough to have a strong influence on the  $T_1$  of **4**. No proton transfer occurs in the dihydrogen bond since this would lead occasionally to dihydrogen elimination and formation of **3**. Breaking of

the dihydrogen bond and rotation of the Cp ligand will allow proton transfer on ruthenium to give a monocationic dihydride, not observed in this system, which is rapidly deprotonated by the amino group before or after Cp rotation. In the latter case the result of the process is a proton/hydride exchange. In the related dppm complexes studied by Lau and co-workers,<sup>13</sup> this process cannot take place and is indeed not observed, whereas the presence of a dihydrogen bond is demonstrated and the transfer of proton is shown to lead to dihydrogen elimination and formation of a chelated species, in agreement with our theoretical results.

In conclusion this study evidences the complexity of a system designed to study one phenomenon, namely, proton transfer within a dihydrogen bond. It demonstrates the presence of multiple pathways for the protons to be transferred to and from the metal, the direct transfer within the dihydrogen bond being high in energy. This result is probably general for proton-transferring systems in which pathways involving solvents or additional functions in the vicinity of the metal must be considered. Finally it shows the strong involvement of ligands in the reactivity of these electrophilic hydride complexes which could be used to transfer protons during catalytic processes. Such possibilities are presently being explored.

## Experimental Section

All manipulations were carried out with standard high-vacuum or dry argon atmosphere techniques. <sup>1</sup>H, <sup>13</sup>C, and <sup>31</sup>P NMR spectra were recorded on a Bruker AC 200, AM 250, or AMX 400 spectrometers. The NMR chemical shifts are reported in ppm, relative to Me<sub>4</sub>Si for <sup>1</sup>H and <sup>13</sup>C and relative to 85% H<sub>3</sub>PO<sub>4</sub> for <sup>31</sup>P.

**Computational Details.** All the calculations were performed with the Gaussian 94 set of programs<sup>19</sup> at the B3PW91 level.<sup>20,21</sup> Ruthenium was represented with the Hay–Wadt relativistic core potential (ECP) for the 28 innermost electrons



and its associated double- $\zeta$  basis set.<sup>22</sup> Phosphorus atoms were also represented with Los Alamos ECPs and the associated double- $\zeta$  basis set<sup>23</sup> augmented by polarization d functions.<sup>24</sup> A 6-31G(d,p) basis set<sup>25,26</sup> was used for the remaining atoms. Full geometry optimizations within  $C_s$  symmetry have been carried out within the framework of DFT(B3PW91).

**Starting Materials.**  $[\text{RuH}(\text{OCOMe})(\text{PPh}_3)_3]$ <sup>14</sup> and the aminocyclopentadienyl ligand<sup>10</sup> were prepared according to published methods.

**(HNEt<sub>3</sub>)(BPh<sub>4</sub>).** (HNEt<sub>3</sub>)(BPh<sub>4</sub>) was obtained from the reaction between NET<sub>3</sub> (1.2 mL) and HCl (37% in water, 1.3 mL) in methanol (20 mL), in the presence of Na(BPh<sub>4</sub>) (5 g) as colorless crystals that were washed twice with methanol and dried in vacuo. Yield: 1.60 g (45%). <sup>1</sup>H NMR (200 MHz, CD<sub>2</sub>Cl<sub>2</sub>): 7.5–6.9 (m, 20 H, BPh<sub>4</sub>); 2.23 (q,  $J_{\text{H-H}} = 7$  Hz, 6 H, HN(CH<sub>2</sub>CH<sub>3</sub>)<sub>3</sub>), 0.87 (t,  $J_{\text{H-H}} = 7$  Hz, 9 H, HN(CH<sub>2</sub>CH<sub>3</sub>)<sub>3</sub>) (the signal of HN(CH<sub>2</sub>CH<sub>3</sub>)<sub>3</sub> is averaged with the water at 1.55 ppm, broad). IR (Nujol) in cm<sup>-1</sup>: 3400, br, NH.

**{HP(n-Bu)<sub>3</sub>}(BPh<sub>4</sub>).** {HP(n-Bu)<sub>3</sub>}(BPh<sub>4</sub>) was obtained from the reaction between P(n-Bu)<sub>3</sub> (3.3 mL) and concentrated HCl (37% in water, 1.3 mL) in methanol (50 mL), in the presence of Na(BPh<sub>4</sub>) (5 g) as colorless crystal that were washed twice with methanol and dried in vacuo. Yield: 4.06 g (53%). <sup>1</sup>H NMR (200 MHz, CD<sub>2</sub>Cl<sub>2</sub>): 7.50–6.90 (m, 20 H, BPh<sub>4</sub>); 3.87 (d of septuplets,  $J_{\text{P-H}} = 488$  Hz,  $J_{\text{H-H}} = 5$  Hz, HP(n-Bu)<sub>3</sub>); 1.6–0.90 (m, 27 H, HP(n-Bu)<sub>3</sub>). <sup>31</sup>P NMR (81.0 MHz, CD<sub>2</sub>Cl<sub>2</sub>): 11.6 (d,  $J_{\text{P-H}} = 488$  Hz). <sup>31</sup>P{<sup>1</sup>H} NMR (81.0 MHz, CD<sub>2</sub>Cl<sub>2</sub>): 11.6 (s). IR (Nujol) in cm<sup>-1</sup>: 2408 (P–H).

**Preparation of [(CpCH<sub>2</sub>CH<sub>2</sub>NMe<sub>2</sub>)RuH(PPh<sub>3</sub>)<sub>2</sub>] (1).** Methanol (35 mL) is added to [RuH(OCOMe)(PPh<sub>3</sub>)<sub>3</sub>] (592 mg; 0.626 mmol) and Na(CpCH<sub>2</sub>CH<sub>2</sub>NMe<sub>2</sub>) (100 mg; 0.626 mmol), and the mixture is heated under reflux for 45 min. During this time the solution clears and a small amount of a yellow precipitate of [RuH<sub>2</sub>(CO)(PPh<sub>3</sub>)<sub>3</sub>] is formed. The yellow suspension is allowed to cool and filtered. The solution is then evaporated to dryness. The residue is extracted with diethyl ether (ca. 20 mL), hexane is added (ca. 15 mL), and the solution is evaporated to approximately half-volume under reduced pressure and allowed to stand at room temperature until crystallization. The supernatant is filtered off, and the yellow crystals are washed twice with pentane and dried in vacuo. Yield: 344 mg (72%). <sup>1</sup>H NMR (200 MHz, CD<sub>2</sub>Cl<sub>2</sub>): 7.50–7.00 (m, 30 H, PPh<sub>3</sub>); 4.27 (t, 1.7 Hz, 2H, C<sub>5</sub>H<sub>4</sub>CH<sub>2</sub>CH<sub>2</sub>NMe<sub>2</sub>), 3.82 (t, 1.7 Hz, 2 H, C<sub>5</sub>H<sub>4</sub>CH<sub>2</sub>CH<sub>2</sub>NMe<sub>2</sub>); 2.30 and 2.02 (m, 4 H, C<sub>5</sub>H<sub>4</sub>CH<sub>2</sub>CH<sub>2</sub>NMe<sub>2</sub>); 2.10 (s, 6 H, C<sub>5</sub>H<sub>4</sub>CH<sub>2</sub>CH<sub>2</sub>NMe<sub>2</sub>); –11.56 (t,  $J_{\text{P-H}} = 34.0$  Hz, 1 H, RuH). <sup>31</sup>P{<sup>1</sup>H} NMR (81.0 MHz, CD<sub>2</sub>Cl<sub>2</sub>): 70.07 (s). <sup>13</sup>C NMR (50.32 MHz, C<sub>6</sub>D<sub>6</sub>): 141.0 (m), 133.74 (d, 161 Hz), 127.77 (d, 160 Hz), 126.79 (d, 159 Hz) (all for PPh<sub>3</sub>); 102.74 (s, quaternary C of C<sub>5</sub>H<sub>4</sub>CH<sub>2</sub>CH<sub>2</sub>NMe<sub>2</sub>); 81.77 (dd, 174 and 6 Hz), 80.43 (d, 175 Hz, C–H of C<sub>5</sub>H<sub>4</sub>CH<sub>2</sub>CH<sub>2</sub>NMe<sub>2</sub>); 63.20 (t, 136 Hz, C<sub>5</sub>H<sub>4</sub>–CH<sub>2</sub>CH<sub>2</sub>NMe<sub>2</sub>), 45.18 (q, 129 Hz, C<sub>5</sub>H<sub>4</sub>CH<sub>2</sub>CH<sub>2</sub>NMe<sub>2</sub>) and 27.29 (t, 127 Hz, C<sub>5</sub>H<sub>4</sub>CH<sub>2</sub>CH<sub>2</sub>NMe<sub>2</sub>). IR (Nujol) in cm<sup>-1</sup>: 1941 (br, Ru–H). Anal. Calcd for C<sub>45</sub>H<sub>45</sub>NP<sub>2</sub>Ru: C, 70.85; H, 5.95; N, 1.84. Found: C, 70.78; H, 6.01; N, 1.78.

(19) Frisch, M. J.; Trucks, G. W.; Schlegel, H. B.; Gill, P. M. W.; Johnson, B. G.; Robb, M. A.; Cheeseman, J. R.; Keith, T.; Peterson, G. A.; Montgomery, J. A.; Raghavachari, K.; Al-Laham, M. A.; Zakrzewski, V. G.; Ortiz, J. V.; Foresman, J. B.; Peng, C. Y.; Ayala, P. Y.; Chen, W.; Wong, M. W.; Andres, J. L.; Replogle, E. S.; Gomperts, R.; Martin, R. L.; Fox, D. J.; Binkley, J. S.; Defrees, D. J.; Baker, J.; Stewart, J. P.; Head-Gordon, M.; Gonzalez, C.; Pople, J. A. *Gaussian 94*, Revision B3; Gaussian Inc.: Pittsburgh, PA, 1995.

(20) Becke, A. D. *J. Chem. Phys.* **1993**, *98*, 5648.

(21) Perdew, J. P.; Wang, Y. *Phys. Rev. B* **1992**, *45*, 13244.

(22) Hay, P. J.; Wadt, W. R. *J. Chem. Phys.* **1985**, *82*, 299.

(23) Wadt, W. R.; Hay, P. J. *J. Chem. Phys.* **1985**, *82*, 284.

(24) Hölwarth, A.; Böhme, M.; Dapprich, S.; Ehlers, A. W.; Gobbi, A.; Jonas, V.; Köhler, K.; Stegmann, R.; Veldkamp, A.; Frenking, G. *Chem. Phys. Lett.* **1993**, *208*, 237.

(25) Hehre, W. J.; Ditchfield, R.; Pople, J. A. *J. Chem. Phys.* **1972**, *56*, 2257.

(26) Harihan, P. C.; Pople, J. A. *Theor. Chim. Acta* **1973**, *28*, 213.

**Preparation of [(CpCH<sub>2</sub>CH<sub>2</sub>NMe<sub>2</sub>)RuH<sub>2</sub>(PPh<sub>3</sub>)<sub>2</sub>](PF<sub>6</sub>)<sub>2</sub> (2).** [(CpCH<sub>2</sub>CH<sub>2</sub>NMe<sub>2</sub>)RuH(PPh<sub>3</sub>)<sub>2</sub>] (50.0 mg, 0.065 mmol) is suspended in methanol (12 mL). Addition of an excess of HPF<sub>6</sub> (60% in water, 0.05 mL, 0.24 mmol) leads to complete dissolution of the starting material and, after 5 min, to the appearance of a new white microcrystalline solid. After 1 h, the precipitate is filtered, washed with methanol (3 × 1 mL), and dried in vacuo. Yield: 40 mg (69%). <sup>1</sup>H NMR (200 MHz, CD<sub>2</sub>Cl<sub>2</sub>): 7.60–7.20 (m, 30 H, PPh<sub>3</sub>); 6.6 (s, 1 H, C<sub>5</sub>H<sub>4</sub>CH<sub>2</sub>CH<sub>2</sub>NMe<sub>2</sub>), 5.08 (t, 2 Hz, 2 H, C<sub>5</sub>H<sub>4</sub>CH<sub>2</sub>CH<sub>2</sub>NMe<sub>2</sub>), 4.81 (t, 2 Hz, 2 H, C<sub>5</sub>H<sub>4</sub>CH<sub>2</sub>CH<sub>2</sub>NMe<sub>2</sub>); 2.99 (m, 2H C<sub>5</sub>H<sub>4</sub>CH<sub>2</sub>CH<sub>2</sub>NHMe<sub>2</sub>); 2.76 (d, 5 Hz, 6 H, C<sub>5</sub>H<sub>4</sub>CH<sub>2</sub>CH<sub>2</sub>NHMe<sub>2</sub>); 1.83 (m, 2H C<sub>5</sub>H<sub>4</sub>CH<sub>2</sub>CH<sub>2</sub>NHMe<sub>2</sub>); –7.37 (t,  $J_{\text{P-H}} = 24$  Hz, 2 H, RuH). <sup>13</sup>C NMR (50.32 MHz, CD<sub>2</sub>Cl<sub>2</sub>): 134.42 (m), 133.52 (d, 162 Hz), 131.41 (d, 162 Hz), 129.11 (d, 162 Hz) (all for PPh<sub>3</sub>); 106.53 (s, quaternary C of C<sub>5</sub>H<sub>4</sub>CH<sub>2</sub>CH<sub>2</sub>NHMe<sub>2</sub>); 91.46 (d, 179 Hz), 90.26 (dd, 182 and 4.5 Hz, C–H of C<sub>5</sub>H<sub>4</sub>CH<sub>2</sub>CH<sub>2</sub>NHMe<sub>2</sub>); 58.55 (t, 140 Hz, C<sub>5</sub>H<sub>4</sub>CH<sub>2</sub>CH<sub>2</sub>NHMe<sub>2</sub>), 43.99 (q, 144 Hz, C<sub>5</sub>H<sub>4</sub>CH<sub>2</sub>CH<sub>2</sub>NHMe<sub>2</sub>) and 22.73 (t, 131 Hz, C<sub>5</sub>H<sub>4</sub>CH<sub>2</sub>CH<sub>2</sub>NHMe<sub>2</sub>). <sup>31</sup>P{<sup>1</sup>H} NMR (81.0 MHz, CD<sub>2</sub>Cl<sub>2</sub>): 60.81 (s). IR (Nujol) in cm<sup>-1</sup>: 1994 (Ru–H). Anal. Calcd for C<sub>45</sub>H<sub>47</sub>F<sub>12</sub>NP<sub>4</sub>Ru: C, 51.24; H, 4.49; N, 1.33. Found: C, 51.18; H, 4.41; N, 1.28.

**Preparation of [(CpCH<sub>2</sub>CH<sub>2</sub>NMe<sub>2</sub>)Ru(PPh<sub>3</sub>)<sub>2</sub>](BF<sub>4</sub>) (3).** HBF<sub>4</sub>·OEt<sub>2</sub> (9.4 μL of a 85% solution in diethyl ether, 52.4 × 10<sup>-3</sup> mmol) is added to a vigorously stirred solution of [(CpCH<sub>2</sub>CH<sub>2</sub>NMe<sub>2</sub>)RuH(PPh<sub>3</sub>)<sub>2</sub>] (1) (40 mg, 52.4 × 10<sup>-3</sup> mmol) in diethyl ether (15 mL), leading to the immediate appearance of a yellow precipitate. The precipitate is filtered, washed twice with diethyl ether, and dried under vacuum. Yield: 95%. <sup>1</sup>H NMR (200 MHz, CD<sub>2</sub>Cl<sub>2</sub>): 7.40–7.10 (m, 30 H, PPh<sub>3</sub>); 4.65 (t, 1.6 Hz, 2 H, C<sub>5</sub>H<sub>4</sub>CH<sub>2</sub>CH<sub>2</sub>NMe<sub>2</sub>), 3.57 (t, 1.7 Hz, 2 H, C<sub>5</sub>H<sub>4</sub>CH<sub>2</sub>CH<sub>2</sub>NMe<sub>2</sub>); 3.26 (t, 6.7 Hz, 2H), 2.50 (t, 6.4 Hz, 2 H, C<sub>5</sub>H<sub>4</sub>CH<sub>2</sub>CH<sub>2</sub>NMe<sub>2</sub>); 2.73 (s, 6 H, C<sub>5</sub>H<sub>4</sub>CH<sub>2</sub>CH<sub>2</sub>NMe<sub>2</sub>). <sup>13</sup>C NMR (50.32 MHz, CD<sub>2</sub>Cl<sub>2</sub>): 139.50 (m), 133.68 (d, 161 Hz), 129.18 (d, 162 Hz), 127.74 (d, 162 Hz) (all for PPh<sub>3</sub>); 92.95 (s, quaternary C of C<sub>5</sub>H<sub>4</sub>CH<sub>2</sub>CH<sub>2</sub>NMe<sub>2</sub>); 82.24 (dd, 175 and 6 Hz), 79.96 (d, 175 Hz, C–H of C<sub>5</sub>H<sub>4</sub>CH<sub>2</sub>CH<sub>2</sub>NMe<sub>2</sub>); 57.33 (t, 149 Hz, C<sub>5</sub>H<sub>4</sub>CH<sub>2</sub>CH<sub>2</sub>NMe<sub>2</sub>), 43.11 (q, 142 Hz, C<sub>5</sub>H<sub>4</sub>CH<sub>2</sub>CH<sub>2</sub>NMe<sub>2</sub>) and 22.01 (t, 126 Hz, C<sub>5</sub>H<sub>4</sub>CH<sub>2</sub>CH<sub>2</sub>NMe<sub>2</sub>). <sup>31</sup>P{<sup>1</sup>H} NMR (81.0 MHz, CD<sub>2</sub>Cl<sub>2</sub>): 64.62 (s). Anal. Calcd for C<sub>45</sub>H<sub>44</sub>BF<sub>4</sub>NP<sub>2</sub>Ru: C, 63.69; H, 5.23; N, 1.65. Found: C, 63.14; H, 5.00; N, 1.66.

**Preparation of 1 + (HNEt<sub>3</sub>BPh<sub>4</sub>).** [(CpCH<sub>2</sub>CH<sub>2</sub>NMe<sub>2</sub>)RuH(PPh<sub>3</sub>)<sub>2</sub>] (1) (8.0 mg; 10.5 × 10<sup>-3</sup> mmol) and (HNEt<sub>3</sub>)(BPh<sub>4</sub>) (4.4 mg; 10.5 × 10<sup>-3</sup> mmol) were loaded in a NMR tube, after which CD<sub>2</sub>Cl<sub>2</sub> was added. After 15 min NMR spectra were recorded at different temperatures. <sup>1</sup>H NMR (200 MHz, 293 K, CD<sub>2</sub>Cl<sub>2</sub>): 7.50–7.00 (m, 50 H, PPh<sub>3</sub>, BPh<sub>4</sub>); 4.57 (t, 1.7 Hz, 2H, C<sub>5</sub>H<sub>4</sub>CH<sub>2</sub>CH<sub>2</sub>NMe<sub>2</sub>), 3.53 (t, 1.7 Hz, 2 H, C<sub>5</sub>H<sub>4</sub>CH<sub>2</sub>CH<sub>2</sub>NMe<sub>2</sub>); 2.35 (m, 2 H), 2.18 (m, 2 H, C<sub>5</sub>H<sub>4</sub>–CH<sub>2</sub>CH<sub>2</sub>NMe<sub>2</sub>); 2.06 (s, 6 H, C<sub>5</sub>H<sub>4</sub>CH<sub>2</sub>CH<sub>2</sub>NMe<sub>2</sub>); 2.42 (q, 7 Hz, 6 H, N(CH<sub>2</sub>CH<sub>3</sub>)<sub>3</sub>), 0.96 (t, 7 Hz, 9 H, N(CH<sub>2</sub>CH<sub>3</sub>)<sub>3</sub>); –0.95 (very br, 2 H, RuH and HNMe<sub>2</sub>CH<sub>2</sub>CH<sub>2</sub>C<sub>5</sub>H<sub>4</sub> coalescence). <sup>1</sup>H NMR (400 MHz, CD<sub>2</sub>Cl<sub>2</sub>), 293 K, 7.50–7.00 (m, 50 H, PPh<sub>3</sub>, BPh<sub>4</sub>); 4.55 (t, 1.7 Hz, 2H), 3.53 (t, 1.7 Hz, 2 H, C<sub>5</sub>H<sub>4</sub>CH<sub>2</sub>CH<sub>2</sub>NMe<sub>2</sub>); 2.36 (m, 2 H), 2.17 (m, 2 H, C<sub>5</sub>H<sub>4</sub>CH<sub>2</sub>CH<sub>2</sub>NMe<sub>2</sub>); 2.06 (s, 6 H, C<sub>5</sub>H<sub>4</sub>CH<sub>2</sub>CH<sub>2</sub>NMe<sub>2</sub>); 2.44 (q, 7 Hz, 6 H, N(CH<sub>2</sub>CH<sub>3</sub>)<sub>3</sub>), 0.97 (t, 7 Hz, 9 H, N(CH<sub>2</sub>CH<sub>3</sub>)<sub>3</sub>); no signal for RuH or HNMe<sub>2</sub>CH<sub>2</sub>CH<sub>2</sub>C<sub>5</sub>H<sub>4</sub>; 273 K, no signal for RuH or HNMe<sub>2</sub>CH<sub>2</sub>CH<sub>2</sub>C<sub>5</sub>H<sub>4</sub>; 253 K, –11.6 (very br,  $T_1 = 170$  ms, RuH); 4.9 (very br, HNMe<sub>2</sub>CH<sub>2</sub>CH<sub>2</sub>C<sub>5</sub>H<sub>4</sub>; 233 K, –11.7 (broad,  $T_1 = 140$  ms, RuH); 4.9 (very br, HNMe<sub>2</sub>CH<sub>2</sub>CH<sub>2</sub>C<sub>5</sub>H<sub>4</sub>; 213 K, –11.72 (t,  $J_{\text{P-H}} = 30$  Hz,  $T_1 = 230$  ms, RuH); 6.0 (very br, HNMe<sub>2</sub>CH<sub>2</sub>CH<sub>2</sub>C<sub>5</sub>H<sub>4</sub>; 193 K, –11.68 (t,  $J_{\text{P-H}} = 30$  Hz,  $T_1 = 780$  ms, RuH); 11.9 (br, HNMe<sub>2</sub>CH<sub>2</sub>CH<sub>2</sub>C<sub>5</sub>H<sub>4</sub>). <sup>31</sup>P{<sup>1</sup>H} NMR (162.0 MHz, CD<sub>2</sub>Cl<sub>2</sub>): 293 K, 66.28 (s); 253 K, 67.9 (s); 233 K, 68.8 (s); 213 K, 70.0; 193 K, 70.43 (s).

**Preparation of 1 + (HPBu<sub>3</sub>BPh<sub>4</sub>).** [(CpCH<sub>2</sub>CH<sub>2</sub>NMe<sub>2</sub>)RuH(PPh<sub>3</sub>)<sub>2</sub>] (1) (10.0 mg; 13.1 × 10<sup>-3</sup> mmol) and {HP(n-Bu)<sub>3</sub>}(BPh<sub>4</sub>) (6.8 mg; 13.0 × 10<sup>-3</sup> mmol) were loaded in a NMR tube, after which CD<sub>2</sub>Cl<sub>2</sub> was added. After 15 min, NMR spectra were recorded at different temperatures. <sup>1</sup>H NMR (400 MHz, CD<sub>2</sub>Cl<sub>2</sub>): 293 K, 7.5–6.9 (m, PPh<sub>3</sub>, BPh<sub>4</sub>); 4.72 (br, 2 H, C<sub>5</sub>H<sub>4</sub>–

CH<sub>2</sub>CH<sub>2</sub>NMe<sub>2</sub>), 3.33 (br, 2 H, C<sub>5</sub>H<sub>4</sub>CH<sub>2</sub>CH<sub>2</sub>NMe<sub>2</sub>); 2.48 (m), 2.31 (m, C<sub>5</sub>H<sub>4</sub>CH<sub>2</sub>CH<sub>2</sub>NMe<sub>2</sub>); 2.09 (s, C<sub>5</sub>H<sub>4</sub>CH<sub>2</sub>CH<sub>2</sub>NMe<sub>2</sub>); 1.37 (m), 0.94 (m, P(n-Bu)<sub>3</sub>), -0.3 (very br, NH and Ru-H, coalescence); 263 K, no signal for NH or Ru-H; 233 K, 11.78 (br, N-H, T<sub>1</sub> = 130 ms), -12.1 (br, Ru-H, T<sub>1</sub> = 130 ms); 213 K, 11.76 (br, N-H, T<sub>1</sub> = 180 ms); -12.11 (t, J<sub>P-H</sub> = 32 Hz, Ru-H, T<sub>1</sub> = 180 ms); 193 K, 11.72 (br, N-H, T<sub>1</sub> = 330 ms); -12.12 (t, J<sub>P-H</sub> = 32 Hz, Ru-H, T<sub>1</sub> = 430 ms). <sup>31</sup>P{<sup>1</sup>H} NMR (162.0 MHz, CD<sub>2</sub>Cl<sub>2</sub>): 293 K, 63.37 (s), no signal observed for P(n-Bu)<sub>3</sub>; 263 K, 63.2 (s, PPh<sub>3</sub>), -29.0 (br, P(n-Bu)<sub>3</sub>); 233 K, 63.2 (s, PPh<sub>3</sub>), -29.4 (br, P(n-Bu)<sub>3</sub>); 213 K, 63.2 (s, PPh<sub>3</sub>); -29.7 (s, P(n-Bu)<sub>3</sub>); 193 K, 63.0 (s, PPh<sub>3</sub>); -29.8 (s, P(n-Bu)<sub>3</sub>).

**Preparation of [(Cp-NH)RuH(PPh<sub>3</sub>)<sub>2</sub>][BPh<sub>4</sub>]·H<sub>2</sub>O (4·H<sub>2</sub>O).** (Cp-NH)RuH(PPh<sub>3</sub>)<sub>2</sub> (30 mg, 0.054 mmol) and HNEt<sub>3</sub>-BPh<sub>4</sub> (17 mg, 0.041 mmol) were mixed in a Shlenck tube, and CH<sub>2</sub>Cl<sub>2</sub> (5 mL) was added. To the resulting yellow solution was added MeOH (5 mL). The volume of the solution was reduced to approximately 5 mL and left to stand at room temperature, thereby inducing precipitation of [(Cp-NH)RuH(PPh<sub>3</sub>)<sub>2</sub>][BPh<sub>4</sub>]·H<sub>2</sub>O as yellow crystals (15 mg, 32%). IR (KBr) in cm<sup>-1</sup>: 3590, 3050, 1977, 1605, 1578, 1478, 1434. Anal. Calcd for C<sub>69</sub>H<sub>68</sub>-BNOP<sub>2</sub>Ru: C, 75.29; H, 6.18; N, 1.27. Found: C, 75.01; H, 6.09; N, 1.33.

**X-ray Analysis.** Data were collected on a Stoe Imaging Plate Diffraction System (IPDS) equipped with an Oxford Cryosystems Cooler Device.

The structures were solved by direct methods (SIR92)<sup>27</sup> and refined by least-squares procedures on *F*<sub>obs</sub>. All hydrogen atoms were located on difference Fourier maps, but they were introduced in calculation in idealized positions (*d*(C-H) = 0.96 Å). Their atomic coordinates were recalculated after each cycle

(27) Altomare, A.; Cascarano, G.; Giacovazzo, G.; Guargliardi, A.; Burla, M. C.; Polidori, G.; Camalli, M. *J. Appl. Crystallogr.* **1994**, *27*, 435.

(28) Carruthers, J. R.; Watkin, D. J. *Acta Crystallogr.* **1979**, *A35*, 698.

(29) Watkin, D. J.; Prout, C. K.; Carruthers, R. J.; Betteridge, P. *CRYSTALS* Issue 10; Chemical Crystallography Laboratory: Oxford, U.K., 1996.

(30) Watkin, D. J.; Prout, C. K.; Pearce, L. J. *CAMERON*; Chemical Crystallography Laboratory: University of Oxford, Oxford, U.K., 1996.

(31) *International Tables for X-ray Crystallography*; Kynoch Press: Birmingham, England, 1974; Vol IV.

of refinement and were given isotropic thermal parameters 20% higher than those of the carbon atoms to which they were attached. The hydride atoms labeled H(1) in each compound and the hydrogen H(2) connected to the nitrogen atom N(1) in **4** were isotropically refined. For both structures all non hydrogen atoms were anisotropically refined, except C(7), C(8), C(9), and N(1) of **1**, for which a disorder has been found and which have been isotropically refined on two sites with a occupancy ratio equal to 0.5. The phenyl rings of the counter-anion present in the structure of **4** have been idealized as rigid groups due to the low observations/parameters ratio. The procedures of least-squares refinement were carried out by minimizing the function  $\sum w(|F_o| - |F_c|)^2$ , where *F*<sub>o</sub> and *F*<sub>c</sub> are respectively the observed and calculated structure factors. A weighting scheme was used in the last refinement cycles, where weights are calculated from the following expression:  $w = [\text{weight}]|1 - (\Delta(F)/6\sigma(F))|^2$ .<sup>28</sup> Models reached convergence with the formulas  $R = \sum(|F_o| - |F_c|)/\sum|F_o|$ , and  $R_w = [\sum w(|F_o| - |F_c|)^2/\sum w(|F_o|)^2]^{1/2}$ .

The calculations were performed with a CRYSTALS program<sup>29</sup> running on a PC, and the drawing of the molecules was realized with the aid of CAMERON.<sup>30</sup> The atomic scattering factors were taken from International Tables for X-ray Crystallography.<sup>31</sup>

Further details on the crystal structure investigation are available on request from the Director of the Cambridge Crystallographic Data Centre, 12 Union Road, GB-Cambridge CB21EZ, U.K., on quoting the full journal citation.

**Acknowledgment.** The authors thank CNRS for support and the European Union within the framework of the Human Capital & Mobility Network on "Localization and Transfer of Hydrogen" for a fellowship to J.A.A. and S.F.S.

**Supporting Information Available:** X-ray structural information for **1** and **4**. An X-ray crystallographic file in CIF format is available. Cartesian coordinates of the optimized structure for **A** (in Å). This material is available free of charge via the Internet at <http://pubs.acs.org>.

OM990301L